Metal-insulator transition in RbC_{60} polymer fulleride studied by ESR and electron-spin relaxation

V. A. Atsarkin, V. V. Demidov, and G. A. Vasneva
Institute of Radio Engineering and Electronics, Russian Academy of Sciences, 103907 Moscow, Russia
(Received 24 February 1997)

The ESR intensity, line shape, and longitudinal electron-spin relaxation in the polymer phase of the RbC_{60} fulleride are investigated in the temperature range $4.2<T<300$ K. Most attention is focused on the metal-insulator transition region (25–50 K). It is found that below 50 K the ESR line can be separated into two Lorentzian components ascribed to conduction electrons and some localized paramagnetic centers (with concentration of about 0.03 per formula unit) with allowance made for the relaxation bottleneck. The decrease of the conduction-electron susceptibility obeys an activation law with the characteristic energy $\Delta/k_B=80\pm10$ K related to the opening of a gap $2\Delta\approx100$ cm^{-1}. The same quantity is found by analyzing both longitudinal and transverse relaxation caused by fluctuations of internal fields with correlation time $\tau_c \propto \exp(2\Delta/k_BT)$. Below 25 K, the temperature dependencies of the linewidth and the relaxation times change abruptly, revealing the development of a new ordered state. The nature of this state is discussed. [S0163-1829(97)06135-3]

I. INTRODUCTION

Among different alkali-metal doped C_{60} materials the recently discovered AC_{60} (A=Rb, Cs) linear polymer phase[1–3] attracted special interest because of its unusual conducting and magnetic properties.[1–11] Below 50 K RbC_{60} undergoes a metal-insulator transition followed by the broadening and dramatic disappearance of the conduction-electron spin resonance (CESR).[1,4,8] In the same temperature range, a steep rise of the T_1/T_2 ratio was found[8] (T_1 and T_2 are the longitudinal and transverse relaxation times); that is typical of the transition from metal to nonconducting state (note that the equality $T_1=T_2$ was definitely proved in the metal phase[11]). From the very beginning such behavior was proposed[1] to be caused by quasi-one-dimensional (1D) conductivity along the polymer $(C_{60})_n$ chains, followed by the transition into the spin-density-wave (SDW) ground state below 50 K. This idea received some support through the optical conductivity data,[4,9] which implied the opening of a typical gap at the Fermi surface. However, the ^{13}C high-resolution nuclear magnetic resonance (NMR) (Refs. 12 and 13) as well as some theoretical calculations,[14] argue against preferential conductivity along the polymer chains, though their magnetic properties are thought to be characteristic of quasi-1D systems.[10]

The nature of the magnetic state of the AC_{60} polymer below the transition temperature still remains unclear. The muon-spin rotation studies[5–7] revealed the existence of quasistatic (on the time scale of a few μs) internal magnetic fields of the order of 5 mT below 20–25 K; it was suggested[6,7] that the magnetic structure has no long-range order and resembles spin glasses (SG's). On the other hand, the measurements of the ^{13}C, ^{87}Rb, and ^{133}Cs NMR linewidths and spin relaxation are consistent with the antiferromagnetic (AF) order,[10] which develops progressively below 25 K.

Thus many questions concerning the low-temperature transition in the AC_{60} polymer phase are still under discussion and need further investigation. This is just the objective of our work. We present here a detailed experimental study of the ESR line shape and electron-spin relaxation in the RbC_{60} polymer.

II. EXPERIMENT

The RbC_{60} samples used for the present study were kindly supplied by L. Forro (École Polytechnique Fédérale de Lausanne, Lausanne); the preparation was described in Ref. 1. The ESR probe consisted of fine RbC_{60} powder (particle size less than 1 μm) mixed with powdered Al_2O_3 to prevent electrical contacts between the fulleride grains. The sample was placed into a Teflon container. No precautions were taken against the atmosphere air. No changes in the ESR spectra and relaxation times were observed on keeping the samples at ambient conditions for two years.

Most of the ESR spectra were taken in the X band using Bruker ER-200. The ESR spin susceptibility (hereafter denoted χ) was measured as the integral intensity of the ESR absorption; the absolute χ values presented in the figures were calibrated by comparing our data with those by Chauvet *et al.*[1] at 300 K.

Temperature was controlled by means of the Oxford cryogenic system and additionally checked against the ESR intensity of a small ruby crystal placed inside the microwave cavity close to the RbC_{60} sample. The accuracy of temperature determination was about 1 K.

The longitudinal electron-spin relaxation time T_1 was measured using an original technique[15] based on directly registering the longitudinal spin magnetization of the sample,

$$M_z(t)=U\sin\Omega t+V\cos\Omega t,$$

under a deep amplitude modulation of the microwave power with the modulation frequency $\Omega\approx10^7$ s^{-1}. Here U and V are the in-phase and out-of-phase components of the magne-

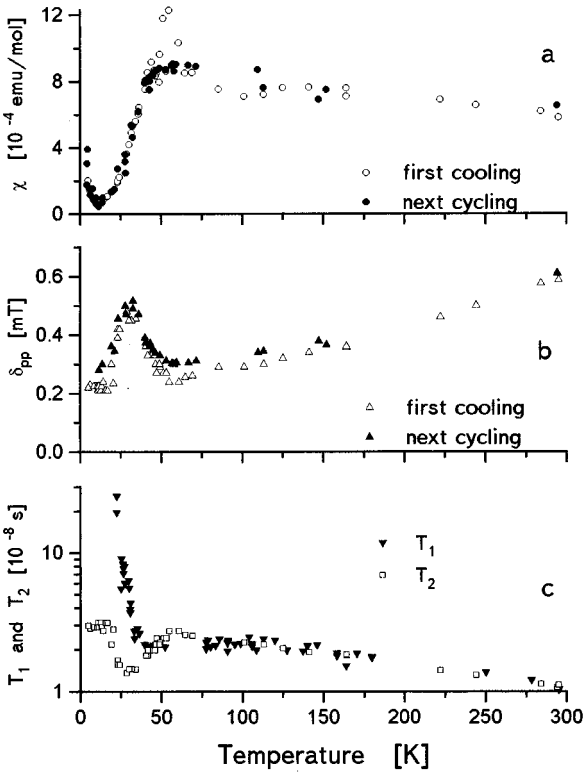

FIG. 1. Temperature dependencies of the integral ESR intensity (a), the peak-to-peak linewidth (b), and the relaxation times (c) of the RbC_{60} polymer.

tization response relative to the modulation wave form. The measurements were carried out by means of the homemade apparatus described previously.[15,16] The ''phase version'' of the method was used, the T_1 value being deduced from the expression

$$\frac{V}{U}=(T_1+\tfrac{1}{2}T_2), \tag{1}$$

where

$$T_2=\left(\frac{\sqrt{3}}{2}\,\gamma\delta_{\rm pp}\right)^{-1} \tag{2}$$

is the transverse relaxation time calculated from the peak-to-peak width $\delta_{\rm pp}$ of the ESR line assumed to be Lorentzian, and γ is the magnetogiric ratio. Experimental details of measuring T_1 are presented elsewhere.[11,15,16]

III. RESULTS

A. General review

Figure 1 shows a general survey of the ESR and relaxation results in the temperature range $4.2<T<300$ K. These data agree qualitatively with those published previously.[1,4,8,11] The integral ESR intensity χ [Fig. 1(a)] increases moderately as temperature decreases from 300 to about 50 K, and then steeply decreases. On further cooling below 10 K the χ value increases again, this time according to the Curie law. The linewidth [Fig. 1(b)] exhibits a pronounced peak near 25 K. Finally, the longitudinal relaxation time T_1 remains equal to T_2 at 45–300 K but strongly increases at lower temperatures where the T_1/T_2 ratio becomes much more than unity, see Fig. 1(c). Note that this figure shows the effective T_2 values calculated using Eq. (2), which is valued only for the Lorentzian line shape. In the next section we shall see that serious corrections are needed in the transition region.

Taken together all these observations are qualitatively consistent with the suggested[1,2] metal-insulator transition accompanied by corresponding loss of the conduction-electron magnetic susceptibility. The low-temperature Curie-like behavior is probably due to some paramagnetic defects or impurities. Note that the Curie-like contribution strongly depends on the particular specimen [compare Fig. 1(a) with other published data[1,4,8]].

Interestingly, some results are found to be dependent on the thermal history. For instance, the χ maximum between 50 and 60 K was more pronounced at the first cooling of a virgin sample than during the succeeding cycles [see Fig. 1(a)]. Besides, a slight irreversible increase of the linewidth has arisen after the first cycling [see Fig. 1(b)], as caused by an additional random field of about 0.18 mT.

B. Detailed description of the transition region

From the accurate analysis of the ESR spectrum we have found that at $T<50$ K the line is no longer single Lorentzian; namely, some additional absorption arises at the distant wings and, besides, the line becomes slightly asymmetric; see Fig. 2. These effects grow progressively down to 25 K, where the maximum linewidth is reached. At this point, however, all these tendencies sharply convert to the opposite ones: the asymmetry changes its sign and then gradually dies out, whereas the linewidth decreases and below 15 K tends to a constant value.

It was found that in the range 25–45 K the line shape can be well fitted by a sum of two Lorentzian components: the ''narrow'' (A) and ''broad'' (B) ones. An example is presented in Fig. 2. The best-fit parameters of both components are plotted against temperature in Figs. 3–5; these are the central results of this paper.

One can see from Fig. 3 that the ''partial'' ESR susceptibilities χ_A and χ_B behave quite differently from each other. As temperature decreases, the χ_A value drops by about an order of magnitude, whereas χ_B to the contrary increases and tends to about one half the initial χ value at 50 K. At the same time both A and B components broaden significantly when cooling from 45 to 25 K, see Fig. 4 [it should be borne in mind that the plotted quantities $(T_2^A)^{-1}$ and $(T_2^B)^{-1}$ are calculated using Eq. (2) and so are proportional to the linewidths]. We consider the A component as caused by the conduction electrons and the B component as related to some localized paramagnetic centers. This suggestion will be discussed in detail in the next section.

Just below 25 K the shape of the ESR line becomes more complicated (see below), but at $T<10$ K the two-line fit is again possible; the resulting components denoted C and D are characterized by Lorentzian forms with the temperature-independent linewidths of 0.4 and 0.2 mT, respectively. Both C and D components obey the Curie law (see Fig. 3) and

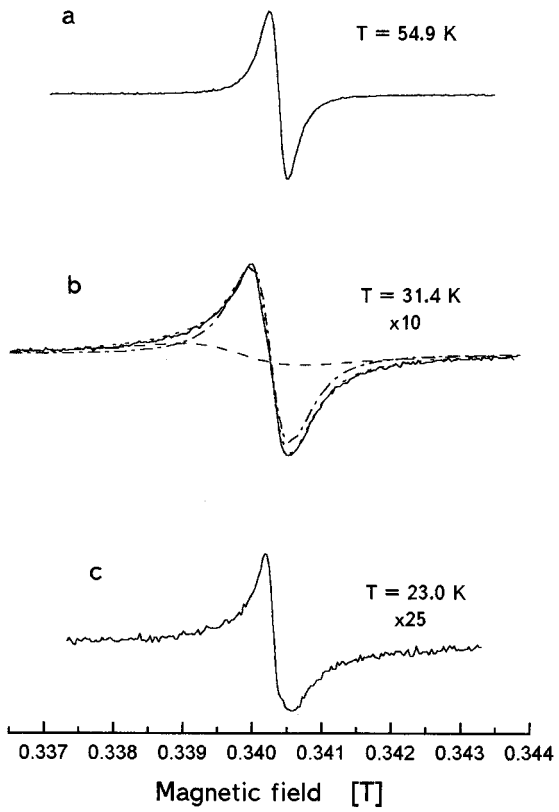

FIG. 2. Variation of the absorption-derivative ESR spectra of the RbC_{60} polymer with temperature. (a) Shows the Lorentzian line shape above the transition. (b) Gives an example of the deconvolution of the observed line (solid curve) into two Lorentzian components: A (dashed-dotted curve) and B (broken curve); the sum of the both is represented by the dotted line. (c) Shows a typical line just below 25 K.

correspond to practically equal spin concentrations of about 1.2×10^{-3} per RbC_{60} formula unit.

Between 15 and 25 K the deconvolution of the ESR line is rather sophisticated and, perhaps, not unique. Nevertheless

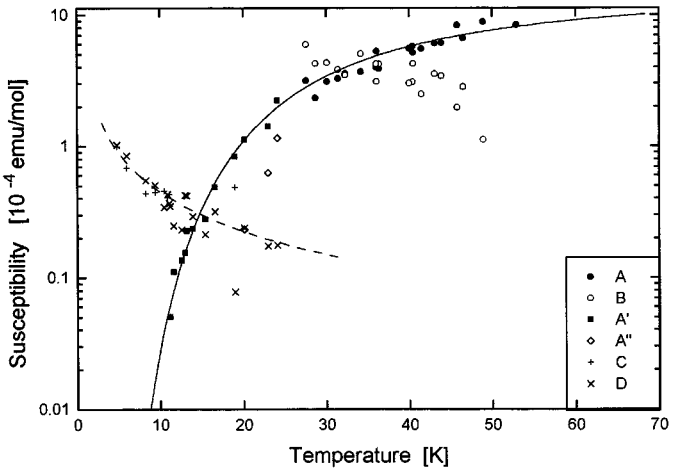

FIG. 3. Integral intensity of the A, B, A', A'', C, and D components separated from the RbC_{60} ESR spectrum vs temperature below the transition point. The solid line represents the activation law, Eq. (3); the broken curve shows the Curie law.

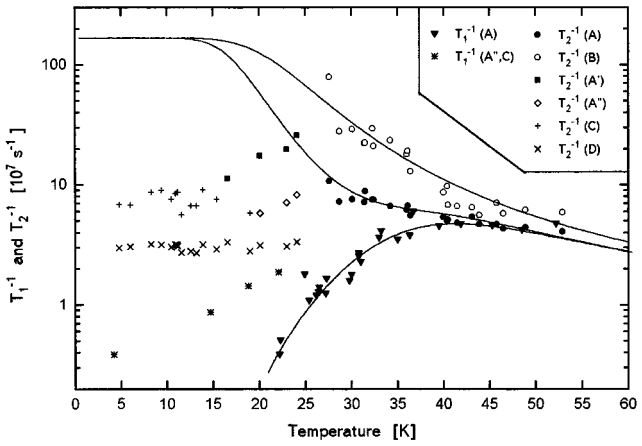

FIG. 4. Longitudinal (T_1^{-1}) and transverse (T_2^{-1}) relaxation rates of the different ESR components plotted against temperature within the transition region. The solid lines represent the fit by Eqs. (8)–(11) with the parameters given by Eq. (12).

we have managed to separate, apart from the Curie-like lines C and D, two other Lorentzian lines denoted A' and A''; both die out upon cooling (Fig. 3). Here the widths and intensities can be estimated only approximately as exemplified by the large scatter of the data points. In the range 10–15 K, the A' and C lines cannot be distinguished from each other because of close widths and g factors (see Figs. 4 and 5); so in this temperature range the $\chi_{A'}$ values shown in Fig. 3 are evaluated by subtracting the Curie-law contribution from the integral ESR intensity.

The longitudinal relaxation rates are presented in Fig. 4. Below 45 K the T_1 data correspond to the narrower (A) ESR component as verified by the field dependence of the magnetization response (for a more detailed description of the technique see Refs. 15, 16, and 11). As to the B component, we can only state that $T_1^B \leqslant T_1^A$. A steep increase of the T_1^A/T_2^A ratio occurs on cooling below 45 K.

The A'' component can be separated only in the narrow temperature range (20–25 K); at $T<20$ K it becomes indistinguishable from the C line (for this reason, the T_1 data for both C and A'' components are indicated in Fig. 4 by the

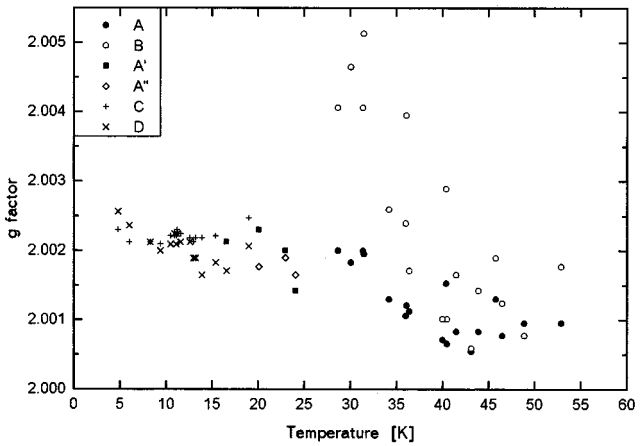

FIG. 5. Temperature dependence of the g factors related to the different ESR components.

same symbols. The origin of the A'' line is not yet clear. Perhaps this signal is related to thermally activated conduction electrons localized in some distorted regions (short polymer chains, etc.) An argument for this explanation might be the fact that the $T_1^{A''}$ value is comparable to (actually it joins smoothly) the conduction electron T_1^A. As to the T_1^D value, it appears to be much more than 10^{-6} s and so cannot be measured by means of the technique employed.

Figure 5 gives temperature dependencies of g factors for all the components of the ESR spectrum mentioned above. The accuracy is rather poor because of strong overlapping of the components, especially within 15–25 K. Nevertheless, the data shown in Fig. 5 are indicative of a noticeable increase of g_B as temperature decreases from 45 to 25 K. In the same temperature range, the g_A value grows a little and then transforms smoothly to $g_{A'}$. The latter observation provides evidence for the similar nature of the A and A' components, whereas the B component apparently has no observable extension below 25 K.

From the general inspection we can summarize the experimental data as follows. The metal-insulator transition in our RbC_{60} samples consists of two stages. The onset temperature T_{c1} is about 50 K, and $T_{c2}=25$ K is another crucial point. Below T_{c1} the ESR intensity starts to decay, the line is separated into two components that broaden with decreasing temperature, and the T_1 value increases. At T_{c2} the transition is over and some new low-temperature state develops that reveals itself in a sharp change of all ESR parameters.

IV. DISCUSSION

Before discussing the physical nature of the transition, we will try to fit our experimental data with reasonable phenomenological expressions. First we shall consider the temperature dependence of χ_A, the intensity of the A component presumably attributed to the delocalized (conduction) electrons. Taking into account that the metal-insulator transition can be accompanied by the opening of an energy gap $E_g=2\Delta$ at the Fermi surface, we test the activation law derived for 1D systems:[17]

$$\chi_A=\frac{\text{const}}{\sqrt{T}}\exp\left(-\frac{\Delta}{k_BT}\right), \tag{3}$$

where k_B is the Boltzmann constant. [Strictly speaking, the temperature dependence of the conduction-electron susceptibility is more complicated;[17] we use, however, the simplest form of Eq. (3), which gives a good approximation at $\Delta>2k_BT$.] The corresponding curve is shown in Fig. 3; note that the points ascribed to the A and A' components are fitted by the same curve supporting the common nature of both the spin species. The best fit is obtained at $\Delta/k_B=80\pm10$ K; this value agrees well with $E_g=100$ cm^{-1} as evaluated from optical conductivity.[4,9]

The next step is to interpret $\chi_B(T)$. In view of the fact that the intensity of the B component increases upon cooling down to 25 K (Fig. 3), this line should be attributed to some localized paramagnetic centers. It is well known that the so-called strong bottleneck can be realized in typical metals.[18] This means that, owing to exchange interaction between the conduction electrons (e) and localized spins (s), their ESR spectra merge into a single Lorentzian line characterized by the averaging of both g factors and relaxation rates weighted with the ''partial'' susceptibilities χ_e and χ_s. The bottleneck conditions (in the ''relaxation mode'') are[18]

$$W_{se},W_{es}\gg W_{sL},W_{eL}. \tag{4}$$

Here W_{se} is the rate of the s-spin relaxation caused by the conduction electrons (the Korringa rate); W_{es} is the rate of the reverse process (the Overhauser relaxation); W_{sL} and W_{eL} are partial spin-lattice relaxation rates of the corresponding spin species. Under even the stronger condition

$$W_{se}\gg\delta_s^0, \tag{5}$$

where δ_s^0 is the partial (for instance, inhomogeneous or dipole-dipole) width of the s spins without the bottleneck, the well-known exchange narrowing should occur that reduces the ''inhomogeneous'' line broadening to[19]

$$\delta^*=\frac{(\delta_s^0)^2}{W_{se}}. \tag{6}$$

We suppose that in the metal phase (above 50 K) Eqs. (4)–(6) are fulfilled. In the course of the metal-insulator transition, however, the W_{se} value, being proportional to $(T\chi_s^2)$, falls off progressively as $\exp(-2\Delta/k_BT)$, see Eq. (3), and inequality (5) starts to break down. We have carefully analyzed this situation by numerical solving of the Bloch-Hasegawa equations;[18,19] the s-spin inhomogeneous ESR broadening δ_s^0 was assumed to be much more than the partial e-spin linewidth W_{eL}. The results of our calculation will be presented in more detail in forthcoming publications and here we restrict ourselves to the main conclusion. It was found that, as the condition of Eq. (5) depresses, the shape of the ESR line ceases to be single Lorentzian and can be approximated by a sum of two Lorentzian curves changing with temperature in fair agreement with our observations for the components A and B. In particular, a temperature range exists where the linewidth of the B component is well described by Eq. (6); so accounting for Eq. (3) one gets

$$(T_2^B)^{-1}=\text{const}\times\exp\left(\frac{2\Delta}{k_BT}\right). \tag{7}$$

Below we shall revert to correlation between this expression and the experimental data.

It is worthwhile to estimate the concentration n_s of the localized s centers in our sample. Assuming that in the metal state χ_e can be approximated by the Pauli susceptibility in the 1D free-electron model with one electron per unit cell[8] and χ_s obeys the Curie law, we get

$$\chi_e^{\text{Pauli}}=\frac{\mu_B^2N_e}{2k_BT_F},\quad \chi_s^{\text{Curie}}=\frac{g^2\mu_B^2N_s}{4k_BT},$$

where μ_B is the Bohr magneton, N_e and N_s are the numbers of the conduction electrons and the s spins, respectively, and T_F is the Fermi temperature. Suppose that at 50 K (above the transition) $\chi_A=\chi_e^{\text{Pauli}}+\chi_s^{\text{Curie}}$, and at 25 K $\chi_B=\chi_s^{\text{Curie}}$. Then, making use of the data of Fig. 3 and supposing[8] $T_F\cong400$ K one can estimate $n_s\approx0.03$ per RbC_{60} formula unit. One might suggest that these paramagnetic centers are

caused by the breaking of the one-dimensional $(C_{60})_n$ polymer chains (similar model was previously applied[20] to paramagnetic fragments of the Cu-O chains in $YBa_2Cu_3O_{6+x}$). In such a case, the mean length of the polymer chain in our RbC_{60} samples is of the order of 30 C_{60} cases; this looks reasonable.

Now we shall pass to the spin relaxation data, Fig. 4. According to general theory,[21] magnetic spin relaxation is due to some time-dependent perturbation commonly considered as a randomly fluctuating internal field with a correlation time τ_c. Within the ''fast motion'' region, where the correlation rate τ_c^{-1} is much more than the fluctuation amplitude, the relaxation times T_1 and T_2 can be written as

$$T_1^{-1}=\langle\delta^2\rangle\,\frac{2\tau_c}{1+\omega_0^2\tau_c^2}, \tag{8}$$

$$T_2^{-1}=\langle\delta^2\rangle\left(a\tau_c+\frac{b\tau_c}{1+\omega_0^2\tau_c^2}\right), \tag{9}$$

where $\langle\delta^2\rangle$ is approximately the second moment of the internal field distribution in the static limit (at $\tau_c\to\infty$); a and b are some factors of the order of unity depending on the specific relaxation mechanism; and ω_0 is the ESR frequency. Since in the very fast motion limit ($\omega_0\tau_c\ll 1$) both relaxation times are equal to each other; one gets from Eqs. (8) and (9), $a+b=2$.

Equations (8) and (9) are representative of the fact that T_1^{-1} is proportional to the spectral density of the correlation function at the resonance frequency ω_0, where T_2^{-1} contains also the zero-frequency contribution represented by the first term in Eq. (9). For the sake of simplicity, the harmonic frequency terms such as $2\omega_0$ are omitted because of their minor effect on the qualitative picture.

One can see from Eq. (9) that at $\tau_c\to\infty$ the transverse relaxation rate diverges. This is caused by the fact that Eqs. (8) and (9) are not valid in the slow-motion limit. Rigorous treatment of this case is very complicated,[22] so we reasonably suggest that in the static limit the T_2^{-1} value tends to $\langle\delta^2\rangle^{1/2}$ (hereafter denoted δ) according to

$$(T_2^{-1})_{\text{corrected}}=(\delta^{-1}+T_2)^{-1}, \tag{10}$$

where T_2 is determined from Eq. (9).

In order to apply Eqs. (8)–(10) to our experimental data, one has to specify the temperature dependence of the correlation time. We assume that τ_c obeys an activation law with some characteristic energy E_a:

$$\tau_c=\tau_c^0\exp\left(\frac{E_a}{k_BT}\right). \tag{11}$$

Three curves calculated from Eqs. (8)–(11) are shown in Fig. 4; at $T>25$ K they fit all the experimental points related to *both* longitudinal and transverse relaxation. It should be emphasized that the agreement is achieved with the *single set* of the main adjustable parameters:

$$E_a/k_B=(150\pm 20)\ \text{K};\quad \tau_c^0=4.5\times 10^{-13}\ \text{s};$$

$$\delta=1.7\times 10^9\ \text{s}^{-1}. \tag{12}$$

As seen, the evaluated activation energy E_a practically coincides with the energy gap $E_g=2\Delta$ deduced above from the $\chi_A(T)$ dependence; see Eq. (3). This is the central finding of our analysis.

As to the a and b factors, the best fit was obtained with $(a=0.4;b=1.6)$ for T_2^A and $(a=2;b=0)$ for T_2^B. In the latter case, Eq. (9) becomes entirely equivalent to Eq. (6), which describes the exchange narrowing of the inhomogeneous line of the s spins under the bottleneck condition. This suggests an idea about the nature of the correlation time τ_c: in fact, the role of τ_c is played by the characteristic time $T_{se}\equiv 1/W_{se}$ of the $s\to e$ scattering. As mentioned above, $T_{se}\propto T\chi_s^2\propto\exp(2\Delta/k_BT)$, so the coincidence of E_a and 2Δ looks quite natural.

Similar identification of τ_c with T_{se} was previously realized within the framework of the bottleneck theory as applied to classical 3D metals;[19] this suggestion was also used in studying ESR and relaxation phenomena in the $(FA)_2PF_6$ organic 1D material (FA is fluoranthene, C_6H_{10}).[23]

The next problem to be discussed is the origin of the ''inhomogeneous'' broadening δ_s^0, which is equivalent to the rms internal field δ in Eqs. (8)–(10). It is just this field that is randomly modulated with the correlation time τ_c leading to both transverse and longitudinal relaxation in the overall spin system. In the case of $(FA)_2PF_6$, this field was proved[23] to originate from the s-e dipole-dipole interaction. The same model could be effective in the RbC_{60} polymer, though our data are not yet sufficient for a certain conclusion.

One more mechanism responsible for τ_c and also governed by the activation energy E_g might be the interband electron hopping. Finally, one could speculate that the motion of the charge carriers destroys the development of the AF correlations along the polymer chains and so produces magnetic fluctuations characterized by the magnitude δ and the correlation time τ_c, in much the same way as it proceeds in the CuO_2 planes of the oxide high-temperature superconductors (for example, see Ref. 24 and references therein). In such a model, T_{c2} might be a critical point where the concentration of the thermally activated conduction electrons becomes too low to prevent magnetic ordering.

We pass to the question of what happens in the RbC_{60} polymer below 25 K. Unlike the previous papers[5–7,10] where the existence of a static magnetic order [either SDW (Ref. 5), SG (Refs. 6 and 7), or AF (Ref. 10)] was strongly supported by NMR and μSR (where SR is spin resonance) observations, our data doesn't yield such unambiguous evidences. On the one hand, the rms internal field estimated in the static limit from Fig. 4 is $\delta/\gamma\cong 10$ mT, in order-of-magnitude agreement with both NMR (Ref. 10) and μSR (Refs. 5–7) results. On the other hand, however, the pronounced line narrowing is observed below 25 K [see Figs. 1(b) and 4] instead of the expected broadening. Such behavior is hardly compatible with any kind of magnetic order associated with strong site-dependent internal fields, whether it be AF, SWD, or SG. Of course we cannot exclude that the most broadened lines (such as B component in Fig. 4 and maybe the antiferromagnetic resonance) are lost below T_{c2} just because of their huge broadening. Besides, our three-line fit in the 15–25 K range might be ambiguous. If, however, the observed line narrowing does really exist, one has to suppose

some nonmagnetic ground state such as a charge-density-wave (CDW) or spin-Peierls (SP) one.

A striking resemblance should be pointed out between our RbC_{60} results and those obtained by Sachs *et al.*[23] on the low-temperature phase of $(FA)_2PF_6$ known as a CDW material. In the latter case, the ESR line was also separated into three components ascribed to different kinds of localized and delocalized spins, including the paramagnetic defects related to broken 1D stacks. Further, on cooling well below $T_c = 186$ K the linewidth passed through a maximum. Finally, the activation energy deduced from the $\tau_c(T)$ dependence was twice the activation energy of the conduction-electron susceptibility. As a result, Sachs *et al.*[23] suggested the crucial role of the paramagnetic defects and definitely ruled out a SDW or AF ordering.

Note that the low-temperature ground state in the RbC_{60} polymer might be strongly influenced by the localized paramagnetic centers, especially if they are related to the mean length of the polymer chains and so can affect the 1D-3D crossover. Evidently, the defect concentration may differ in various RbC_{60} samples leading to scatter in experimental results. As an instructive analogy we refer to observation of the AF-SP crossover controlled by external pressure in the $(TMTTF)_2PF_6$ organic conductor.[25]

In conclusion, we have investigated the ESR intensity, line shape, and relaxation behavior in the RbC_{60} polymer in the range of the metal-insulator transition. Two critical points are found, $T_{c1} = 50$ K and $T_{c2} = 25$ K. Below T_{c1} two components of the ESR spectra have been extracted and identified as being due to conduction electrons and localized paramagnetic defects. The activation energy $\Delta/k_B \cong 80$ K of the conduction-electron susceptibility is found; this value is supported by the activation behavior of the correlation time τ_c governing both transverse and longitudinal relaxation under the bottleneck condition. From these data, the energy gap E_g in the insulating state is estimated as $2\Delta \cong 100$ cm^{-1}. A sharp change in the ESR parameters below 25 K suggests a transition to some ordered state; however, the ESR data are not yet sufficient to make an ultimate conclusion on its nature, so further study is needed.

ACKNOWLEDGMENTS

We are greatly indebted to L. Forró and A. Jánossy for kindly supplying the RbC_{60} samples for this study. We thank N. Kirova, A. Smirnov, S. Artemenko, and S. Zaitsev-Zotov for helpful discussions. The work was supported by the Russian State Foundation for Basic Research, Grant No. 96-02-19719.

[1] O. Chauvet, G. Oszlànyi, L. Forró, P. W. Stepnens, M. Tegze, G. Faigel, and A. Jánossy, Phys. Rev. Lett. **72**, 2721 (1994).
[2] P. W. Stephens, G. Bortel, G. Faigel, M. Tegze, A. Jánossy, S. Pekker, G. Oszlànyi, and L. Forró, Nature (London) **370**, 636 (1994).
[3] S. Pekker, L. Forró, L. Mihály, and A. Jánossy, Solid State Commun. **90**, 349 (1994).
[4] F. Bommeli, L. Degiorgi, P. Wachter, Ö. Legeza, A. Jánossy, G. Oszlànyi, O. Chauvet, and L. Forró, Phys. Rev. B **51**, 14 794 (1995).
[5] Y. J. Uemura, K. Kojima, G. M. Luke, W. D. Wu, G. Oszlànyi, O. Chauvet, and L. Forró, Phys. Rev. B **52**, R6991 (1995).
[6] W. A. MacFarlane, R. F. Kiefl, S. Dusinger, J. E. Sonier, and J. E. Fischer, Phys. Rev. B **52**, R6995 (1995).
[7] L. Cristofolini, A. Lappas, K. Vavekis, K. Prassides, R. DeRenzi, M. Ricco, A. Schenk, A. Amato, F. N. Gypax, M. Kosaka, and K. Tanigaki, J. Phys. Condens. Matter **7**, L567 (1995).
[8] J. Robert, P. Petit, J.-J. André, and J. B. Fischer, Solid State Commun. **96**, 143 (1995).
[9] F. Bommeli, L. Degiorgi, P. Wachter, and L. Forró, Synth. Met. **77**, 111 (1996).
[10] V. Brouet, H. Alloul, Y. Yoshinari, and L. Forró, Phys. Rev. Lett. **76**, 3638 (1996).
[11] V. A. Atsarkin, V. V. Demidov, G. A. Vasneva, A. Jánossy, O. Chauvet, and L. Forró, Solid State Commun. **98**, 977 (1996); **98**, 927 (1995).
[12] K.-F. Thier, G. Zimmer, M. Mehring, and F. Rachdi, Phys. Rev. B **53**, R496 (1996).
[13] H. Alloul, V. Brouet, E. Lafontaine, L. Malier, and L. Forró, Phys. Rev. Lett. **76**, 2922 (1996).
[14] S. C. Erwin, G. V. Krishna, and E. J. Mele, Phys. Rev. B **51**, 7345 (1995).
[15] V. A. Atsarkin, V. V. Demidov, and G. A. Vasneva, Phys. Rev. B **52**, 1290 (1995).
[16] V. A. Atsarkin, G. A. Vasneva, and V. V. Demidov, Zh. Eksp. Teor. Fiz. **108**, 927 (1995) [JETP **81**, 509 (1995)].
[17] D. C. Johnston, Phys. Rev. Lett. **52**, 2049 (1984).
[18] S. E. Barnes, Adv. Phys. **30**, 801 (1981).
[19] L. R. Tagirov and K. F. Trutnev, Zh. Eksp. Teor. Fiz. **86**, 1092 (1984) [JETP **59**, 638 (1984)].
[20] J. Sichelschmidt, B. Elschner, A. Loidl, and B. I. Kochelaev, Phys. Rev. B **51**, 9199 (1995).
[21] A. Abragam, *The Principles of Nuclear Magnetism* (University Press, Oxford, 1961).
[22] N. N. Korst and L. I. Antsiferova, Usp. Fiz. Nauk **126**, 67 (1978) [Sov. Phys. Usp. **21**, 761 (1978)].
[23] G. Sachs, E. Pöhlmann, and E. Dormann, J. Magn. Magn. Mater. **69**, 131 (1987).
[24] M. Mehring, Appl. Magn. Reson. **3**, 383 (1992).
[25] G. Caron, F. Creuzet, P. Butaud, C. Bourbonnais, D. Jérôme, and K. Bechgaard, Synth. Met. **27**, B123 (1998).